A microscale photovoltaic neurostimulator for fiber optic delivery of functional electrical stimulation

2007 J. Neural Eng. 4 213

(http://iopscience.iop.org/1741-2552/4/3/006)

IOP Publishing Journal of Neural Engineering

J. Neural Eng. **4** (2007) 213–218 doi:10.1088/1741-2560/4/3/006

A microscale photovoltaic neurostimulator for fiber optic delivery of functional electrical stimulation

Yoon-Kyu Song[1], John Stein[2], William R Patterson[1], Christopher W Bull[1], Kristina M Davitt[1], Mijail D Serruya[1,2], Jiayi Zhang[3], Arto V Nurmikko[1,3] and John P Donoghue[2]

[1] Division of Engineering, Brown University, Providence, RI 02912, USA
[2] Department of Neuroscience, Brown University, Providence, RI 02912, USA
[3] Department of Physics, Brown University, Providence, RI 02912, USA

E-mail: Arto_Nurmikko@brown.edu

Received 31 October 2006
Accepted for publication 26 March 2007
Published 27 April 2007
Online at stacks.iop.org/JNE/4/213

Abstract

Recent advances in functional electrical stimulation (FES) show significant promise for restoring voluntary movement in patients with paralysis or other severe motor impairments. Current approaches for implantable FES systems involve multisite stimulation, posing research issues related to their physical size, power and signal delivery, surgical and safety challenges. To explore a different means for delivering the stimulus to a distant muscle nerve site, we have elicited *in vitro* FES response using a high efficiency microcrystal photovoltaic device as a neurostimulator, integrated with a biocompatible glass optical fiber which forms a lossless, interference-free lightwave conduit for signal and energy transport. As a proof of concept demonstration, a sciatic nerve of a frog is stimulated by the microcrystal device connected to a multimode optical fiber (core diameter of 62.5 μm), which converts optical activation pulses ($\sim$100 μs) from an infrared semiconductor laser source (at 852 nm wavelength) into an FES signal.

(Some figures in this article are in colour only in the electronic version)

Introduction

The most common form of neurostimulation prosthetics uses electrical stimulation to initiate action potentials in nerve fibers that in turn cause chemical neurotransmission to other neurons or end organs such as muscles. These systems can be used to restore hand grasp and release in quadriplegia, standing and stepping in paraplegia, gluteal stimulation to prevent pressure ulcers, restoration of bladder function (continence and micrturition) following spinal cord injury and phrenic pacing of respiration in high-level quadriplegia [1]. Functional electrical stimulation (FES) generally refers to the branch of neurostimulation in which skeletal muscles are stimulated to restore voluntary movement in patients with paralysis or other severe motor impairments. Neurostimulation can be achieved with skin-penetrating percutaneous electrodes or with chronically implanted electrode arrays. FES systems have been shown to improve range of motion, effective muscle strength and the ability to achieve activities of daily living independently in both adults and children implanted with these systems [1, 2].

With recent advances in cortical recording by microelectrode arrays, including early human trials [3], it is becoming possible to envision a future implantable microsystem where neural signals from the cortex are directly linked with muscle nerve sites in the peripheral nervous system (and vice versa). One possible choice for implementing such communication link between cortical and peripheral sites within the body is a glass-based optical fiber, which is biocompatible, mechanically robust and free of electromagnetic interference. Optical fibers could, in principle, be configured as a networked neural communication

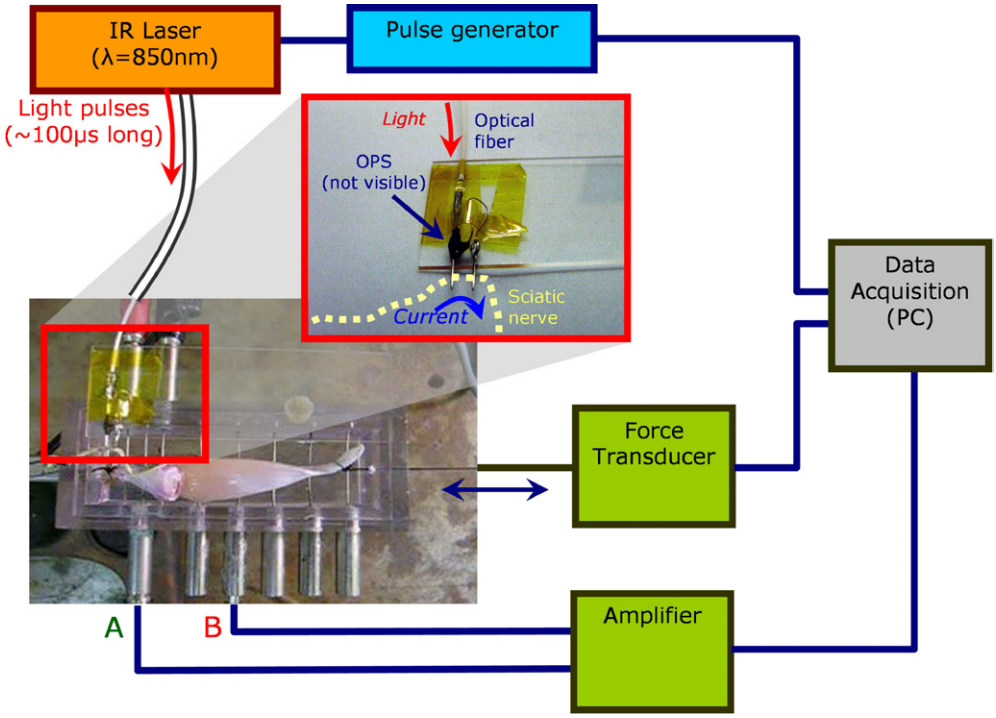

Figure 1. Experimental setup of muscle compound action potential and force measurement (for details see the text); A (reference) and B (recording) are Ag/AgCl electrodes.

system to access multiple sites with a very large total bandwidth for information content, in analogy with fiber optical telecommunication.

In our recent work, we have been developing an integrated cortical neuroprobe where analog electrical signals recorded from the motor cortex by a microelectrode array are extracted as a high data rate digital infrared optical signal, which can be guided into an optical fiber [4, 5]. In this paper, we explore localized peripheral neural activation by launching pulsed infrared light into an optical fiber which is terminated by a high efficiency microscale photovoltaic light-to-current converter chip. As an initial demonstration *in vitro*, a sciatic nerve of a frog is readily stimulated in a standard neuromuscular experiment by converting pulses from an infrared semiconductor laser source (at 852 nm wavelength) into an effective FES drive.

Materials and methods

Tissue preparation

Two adult bullfrogs (*Rana catesbeiana*) weighing 30–40 g were obtained from a commercial supplier. Animals were maintained in an Association for Assessment and Accreditation of Laboratory Animal Care, National Institutes of Health (AAALAC, NIH) approved animal care facility. After the frog was decapitated, one lower limb was dissected from the body. The skin was then dissected off the leg to reveal the muscles and nerves. While remaining attached to the leg muscles distally, the sciatic nerve was identified, and gently excised such that it could be laid without stretching over six Ag/AgCl wire electrodes in a 5 cm × 15 cm Plexiglas nerve chamber, as shown in the photograph in figure 1. The space between the electrodes was 0.5 cm. The proximal end of the frog leg was fixed in place on one end of the chamber and the distal end was attached to a force transducer for later force measurement. A Ringer's saline solution (111.87 mM NaCl, 2.47 mM KCl, 1.08 mM $CaCl_2$ and 2.38 mM $NaHCO_3$) was periodically applied along the length of the nerve to keep it moist.

Photovoltaic microchip converter

The design of the photovoltaic microchip was based on pn-junction gallium-arsenide/aluminum-gallium-arsenide (GaAs/AlGaAs) heterostructures. To achieve an electrical output in terms of both voltage and current parameters of up to several volts and tens of mA from a device with a diameter on the scale of an optical multimode fiber (here ~300 μm), it is necessary to consider a tandem junction design similar to those employed in very high efficiency solar cells [6–8]. Our tandem structure consisted of three p–i–n photovoltaic cells with different intrinsic layer thicknesses connected in series by two thin tunnel junctions. The first photovoltaic cell absorbs one-third of the incident photons, the second cell absorbs the half of the transmitting photons, that is another third of the total photons and the third cell absorbs the rest. Major improvements in the efficiency of such solar cells result from careful design of the layered heterostructures and the growth of high quality single crystal epitaxial thin films [9]. Although the photovoltaic microchip device used in our work converts *monochromatic* light rather than a broad solar spectrum to electrical energy, a carefully designed and balanced multi-junction tandem structure similar to a tandem solar cell is still

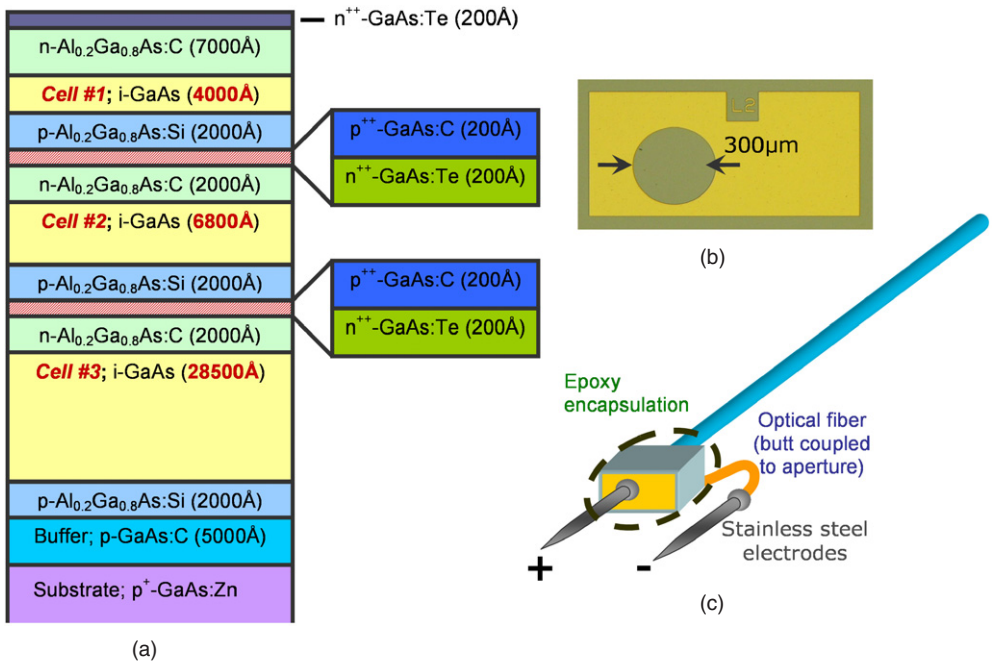

Figure 2. (a) Cross-sectional layering schematic for the photovoltaic microcrystal. (b) Optical microscope image of photovoltaic cell in top view, showing the 300 μm diameter optical window for incident infrared light. (c) Photovoltaic microchip packaging scheme with electrodes.

required to reach maximum theoretical voltage as well as high conversion efficiency.

By employing semiconductor device physical modeling tools, we designed a 15-layer epitaxial thin film structure shown in figure 2(a) which was custom grown on a GaAs substrate wafer using metal organic vapor phase epitaxy (MOVPE) by IQE Inc. (Wales, UK). The tandem device is an n-on-p structure grown on ⟨1 0 0⟩ oriented p^+-GaAs ($[Zn^{2+}] \sim 10^{19}$ cm^{-3}). The epitaxial layers consist of three $Al_{0.2}Ga_{0.8}As$–GaAs–$Al_{0.2}Ga_{0.8}As$ p–i–n photocells with optimally designed thicknesses for a balanced absorption, in which each junction absorbs exactly one-third of incident monochromatic light at the predetermined wavelength of 852 nm (produced by a matched semiconductor laser source), vertically stacked and serially connected by two heavily doped (carbon for p^{++} and tellurium for n^{++}) GaAs tunnel junctions. Circular devices with an n-type ring contact around the aperture were fabricated using evaporated Pd/Ge/Au (100 Å/500 Å/1200 Å) metallization layers. An Ohmic back contact to the p-type substrate was formed with Ti/Au (100 Å/1500 Å) metallization layers. Both contacts were subsequently annealed at 300 °C for 5 min under a forming gas ambient. Various sized apertures (50–300 μm) were formed using standard microelectronic process techniques (see the microphotographic image in figure 2(b)). For a fiber-guided stimulation system, a standard ~60 μm core multimode silica fiber with a total external diameter of approximately 300 μm (including polymer cladding) was attached perpendicular to the entrance window of the photovoltaic device by UV curable epoxy (NOA78, Norland Products, Inc.), after precise alignment to the aperture as the power conversion efficiency was monitored continuously. Following attachment

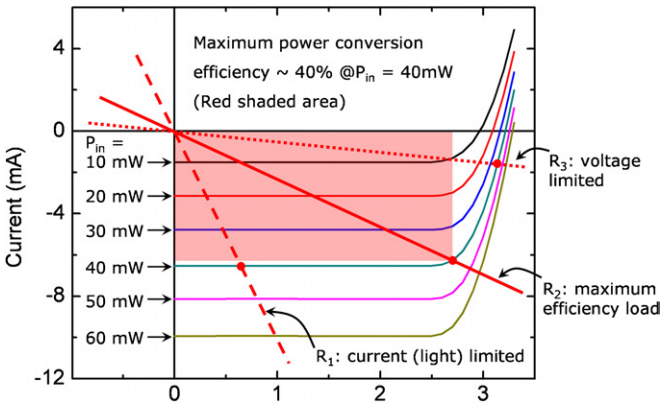

Figure 3. Current–voltage characteristics and performance of the high-efficiency photovoltaic microchip. Three lines represent three different load conditions for the device under a certain amount (40 mW) of laser illumination, showing current (light) limited operation with low impedance load (R_1), voltage (bandgap) limited operation with high impedance load (R_3).

of two stainless steel microelectrodes to the microcrystal device, the entire assembly except the tips of the two electrodes was encapsulated with an epoxy (H70E-4, Epoxy Technology, Inc.) for electrical and environmental isolation (shown schematically in figure 2(c)).

Shown in figure 3 is the current–voltage performance (I–V characteristics) of a typical device under various illumination levels from input laser power $P = 10$ mW up to 60 mW. For $P = 40$ mW, the open circuit voltage is approximately 3.2 V and the short circuit current density is approximately 6.5 mA. The maximum energy conversion efficiency of the device is above 40%, a figure of merit higher than many published values

for other three-junction tandem cells. Such high conversion efficiency is attributed to the design of the photovoltaic multilayer material, the quality of its epitaxial growth as well as careful device fabrication and process control. By depositing a single-layer anti-reflection coating on the aperture window, we expect the intrinsic power conversion efficiency to be extendable readily to at least 50%, an important issue for an implantable device candidate where the unconverted light is dissipated as heat in the surrounding body tissue (characteristics of the photovoltaic device themselves are also affected by the increased temperature, but it is much more tolerant than surrounding tissues). We emphasize here the capability of the high performance microcrystal device to project significant total electrical power which could be used, e.g., to stimulate multiple peripheral or cortical neural sites—in the case of the experiments performed here, only a fraction of such power was in fact required ($P \sim$ 1–2 mW). Also, the photovoltaic device is designed to mimic an ideal current source in a relatively wide range of load impedance. A typical source impedance of the photovoltaic device is several mega ohms or more, depending on the geometry of the device. As shown in figure 3, as long as the load impedance is kept below the maximum efficiency load (R_2), the device demonstrates current (light) limited operation (R_1), but if the load exceeds the maximum efficiency load, it shows voltage (bandgap) limited operation (R_3). If a higher voltage is required, one could imagine stacking more cells with more tunnel junctions, up to a certain point mainly limited by the material growth complexity.

Neuromuscular recording setup

The output from the laser was guided through an optical fiber into the photovoltaic microchip, whose output contacted the sciatic nerve directly at the proximal end of the gastrocnemius muscle. Muscle compound action potentials (CAPs) were recorded differentially from the two most distal probe electrodes of the six Ag/AgCl wire electrode testbed using a National Instruments stimulator-A/D converter unit, and saved with a custom LabView program. The neuromuscular response was measured simultaneously by a force transducer securely tied to the Achilles tendon at the distal end of gastrocnemius muscle, and the data were recorded using the same computer system.

Optical functional electrical stimulation modalities

For fiber optic guided experiments, a multimode optical fiber (62.5 μm core diameter) was used to deliver the laser energy to the optical functional electrical stimulation assembly, as shown in figure 1. Pulsed input laser power was attenuated to $P =$ 2 mW or less, just sufficient for unambiguous neuromuscular response, by adjusting the amount of injection current through a commercially available pulsed GaAs diode laser (SRT-F850S-60, Micro Laser Systems, Inc.). Laser power was measured with a calibrated powermeter (OMM 6810B, ILX Lightwave Cooperation). Laser operating parameters were as follows: wavelength, 852 nm; pulse duration, 100 μs; and peak power per pulse, 2 mW. The stimulation patterns were

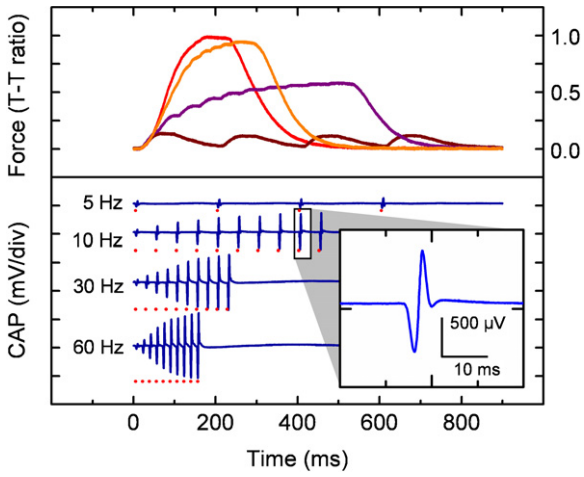

Figure 4. Muscle compound action potential and force measurement of fiber optic guided functional electrical stimulation of the sciatic nerve of the gastrocnemius muscle. The upper panel shows force measurement in T–T ratio (twitch–tetanus ratio) and the lower panel shows muscle compound action potential (CAP) with the detail of a typical waveform as an inset. Red dots under each CAP trace represent timing of individual laser pulses (100 μs long, $P_{\text{laser}} \sim$2 mW). Only four representative frequencies (pulsed laser repetition rate) are shown here.

short bursts of pulses, which varied in the repetition rate and total number of pulses. The pulse repetition rates of 5 Hz, 10 Hz, 20 Hz, 30 Hz, 40 Hz, 50 Hz and 60 Hz were used with four pulses for the 5 Hz case, five for 10 Hz, and ten for the 20 Hz, 30 Hz, 40 Hz, 50 Hz and 60 Hz trains. The sciatic nerve was stimulated by monophasic excitatory current flow between the two stainless steel microelectrodes (cathode proximal and anode distal along the nerve length). A schematic and photographic images of the experimental arrangement are shown in figure 1.

Experimental results

A brief summary of the results is presented in figure 4, which displays the muscle compound action potential and force measurements performed by using the output from the photovoltaic microcrystal device as the externally applied stimulus for the fiber optic delivery of laser light. As shown in figure 4, stimuli at 5 Hz evoked discrete and separate twitches with rapid increase and relatively slower decrease in force. For a 10 Hz pulsed repetition rate, the force did not return to baseline before the second stimulation was evoked, resulting in successive twitches as a cumulatively (integrated) increasing amplitude. By increasing the stimulation frequencies to 20 Hz, 30 Hz and 40 Hz, the mean value of the forces increased correspondingly. Even so, distinct ripples representing individual muscle twitches are still recognizable. Stimulations at 50 Hz and 60 Hz resulted in greater mean forces with fused tetanus and similar latency. These active force responses are characteristic of those observed in standard neuromuscular experiments [10], and thus demonstrate directly the proof of principle and versatility of our microscale optical neurostimulator device. The data show

that the amplitude of the muscle CAPs increased when the stimulation frequencies were increased. This occurred mainly because of the change in the positions of recording contacts. In the case of a weak twitch at 5 Hz, there was a little difference in the action potentials since there was very little physical displacement of the muscle. By contrast, for tetanus of 20 Hz or higher, the muscle motion induced a change in the positions on the recording electrodes, hence reflecting a larger amplitude of action potential. The detail of a muscle compound action potential waveform from a single optical pulse is shown in the inset of figure 4, exhibiting a typical potential profile expected from a differential recording of compound action potential. Slight shift in baseline is mainly attributed to the muscle contraction.

In the case of the experiments where the photoexcitation was not guided by optical fiber but traveled through 'free space', we biased the driving laser diode for higher power and flood illuminate (a few centimeter diameter in area) the photovoltaic device without focusing, in order to roughly simulate the situation with heavy scattering of light in a tissue. These experiments also readily produced a CAP response with muscle dynamics quite similar to those obtained in the fiber optic guided measurements. The 'free space' delivery of light could enable transcutaneous delivery of functional electrical stimulation in specific circumstances.

Discussion and conclusion

In this section we comment on our experimental proof-of-concept demonstration of 'optical functional electrical stimulation', and try to place this possible new technique in perspective with more established contemporary approaches that share some commonality of technical purpose.

Device performance of microcrystal photovoltaic converter

The minimum optical power required to elicit muscular contraction using the fiber optic guide scheme was relatively low, mainly due to the high optical-to-electrical power conversion efficiency of the microcrystal photovoltaic device. Also, with a moderate ($\sim$2 mW) peak optical power at the repetition rate of 60 Hz, a clear tetanus contraction of muscle was measured by the force transducer. We also demonstrated free space optical activation of an ultra compact neurostimulator with the entire volume of the microcrystal device occupying less than 1 mm^3 volume, including complete encapsulation. In this case, the required optical power level was higher due to the small optical cross-section of the device in the absence of any focusing optics. Nonetheless we achieved muscle activation characteristics comparable to the fiber optic guided device, suggesting the potential application of microcrystal devices as superficial infrared optically accessible neuromuscular activators without any tethers.

The present microcrystal with a $\sim$300 μm optical aperture is capable of delivering considerably higher pulses and continuous powers, for example, to serve as the 'power plant' for multielectrode and multisite stimulating microelectrode arrays. The device is inherently very fast (on 10^{-9} timescale, limited by the depletion and parasitic capacitances), so that it would be able to deliver high speed digital command stream for a microelectronic device which might be employed in distributing the electrical stimulation according to spatio-temporal algorithms in a multielectrode system.

Practicality, biocompatibility and surgical issues of an 'optical-FES' system

In terms of possibilities of using infrared light as a means of delivering energy to a local muscle site for actuating functional electrical stimulation for eventual clinical applications, we briefly consider the advanced implanted FES systems already in clinical trials and use [1, 2]. These impressive systems typically employ inductive or percutaneous power and/or signal transmission and telemetry in conjunction with subcutaneous electrical wiring to connect a (programmable) stimulation driver to multiple peripheral nerve sites. For example, Durand and co-workers have recently developed new types of multielectrode arrays applied to multisite stimulation of muscle nerves [11]. In general, muscular contraction can be induced by stimulating the neural circuit at various locations, i.e. electrodes can be placed at the motor point, along the peripheral nerve as it courses through the limb, at the spinal roots or in the spinal cord itself. Each of these locations pose different surgical and stimulation challenges, and generate different sets of advantages and disadvantages in terms of restoring functional movement. To access many distinct and spatially separate sites by cabling via a network of conductive wires may lead to complications, as they may serve as antennae to ambient electromagnetic interference (EMI), experience capacitive coupling or other electrical interactions with other devices, such as cardiac pacemakers, also implanted in the body, or electronics worn externally. In the worst case, metal leads pose the risk of diathermy (thermal damage from increased current induced through the leads). Extensive wiring may also render patients unable to participate in certain diagnostic procedures such as MRI or may cast shadows or other artifacts in certain radiological imaging procedures. Using fiber optic cables in conjunction with microcrystal energy converters may offer an alternative signal and power distribution system where replacing the leads with nonmetallic optical fibers could address such EMI and radiological artifact safety issues. In addition, optical fibers may be more biostable, resilient and biocompatible relative to the saline environment of the body compared to metal leads. Beyond the simple demonstration of this paper, we envision the fiber-based approach to be useful also in cases where programmable microelectronic chips are integrated to the local microelectrode arrays.

There are some other practical considerations in order to use the photovoltaic devices as a neurostimulator in clinical applications. In order to accomplish a safe, charge balanced stimulation of a nerve, one should consider a biphasic implementation of the stimulation with a photovoltaic device. As alluded in the previous section, various types of waveforms including charge balanced biphasic pulses could be implemented with the photovoltaic power plant scheme where

the device serves as a power and signal supplier to a compact IC to generate an arbitrary, eventually multisite waveform. As a simpler implementation, one could also imagine a dual photovoltaic device in a back-to-back diode connection with a multicore fiber to generate the biphasic pulse.

Another important consideration of the device in clinical application is a thermal effect of the scattered or 'unconverted' laser on tissue. Any laser induced heating in our approach is mainly dependent on the conversion efficiency of the photovoltaic device. With efficiencies in the 50% range, and given the optical powers cited above in conjunction with the microcrystal volume, any residual heating generated by the device is estimated to be negligible near 850 nm.

Finally, as for the safety hazards associated with the GaAs microcrystal semiconductor material, while toxicology studies have mainly addressed the inhalation of fine GaAs dust in rats and mice [12], the compound itself is chemically quite stable. The small volume of our microcrystal device requires robust encapsulation in any event, for its functioning in the body–electrolyte environment, not unlike encapsulated batteries ubiquitous in cardiac and neurostimulation devices which can contain toxic heavy metals. Due to the size and process compatibility issue, an encapsulation with soft materials (organic polymers or organic–inorganic composites) is required for the long-term reliability of the device as well as the clinical safety of the host. Some materials in this category have been proposed [13], but it remains as a subject of active research topic.

Conclusion

As a proof of concept demonstration, the sciatic nerve of a frog was stimulated by a photovoltaic neurostimulator connected to a multimode optical fiber, converting optical activation pulses from an infrared semiconductor laser source into an FES signal. Compound neuromuscular potential and muscle contraction force were measured simultaneously to ensure the correlation of the neuromuscular activities with pulsed optically initiated activation. Since our simple, initial platform is readily scalable, we can envision a network of our compact neurostimulators with their superfine optical fiber wiring to provide eventually an assistive *artificial optical nervous system* for advanced neuromotor prosthesis, where the fiber optic wiring may eventually allow a direct communication link from the cortex to a distant muscle site.

Acknowledgments

The research is supported by the ONR (grant no N0014-04-1-082) and the NSF (Biophotonics grant no BES-0423566).

Supplementary information showing a short video clip of the experimental demonstration is available at http://nurmikko.engin.brown.edu/~jiayi/FES/.

References

[1] Grill W M and Kirsch R F 2000 Neuroprosthetic applications of electrical stimulation *Assist. Technol.* **12** 6–20
Heilman B P, Audu M L, Kirsch R F and Triolo R J 2006 Selection of an optimal muscle set for a 16-channel standing neuroprosthesis using a human musculoskeletal model *J. Rehabil. Res. Dev.* **43** 273–85

[2] Davis S E, Mulcahey M J, Smith B T and Betz R R 1999 Outcome of functional electrical stimulation in the rehabilitation of a child with C-5 tetraplegia *J. Spinal Cord Med.* **22** 107–13

[3] Hochberg L R, Mukand J A, Friehs G M and Donoghue J P 2005 BrainGate neural interface system: feasibility study of a human neuromotor prosthesis *Neurology* A **64** (Suppl.) 356–56

[4] Patterson W R, Song Y K, Bull C W, Ozden I, Deangellis A P, McKay J L, Nurmikko A V, Donoghue J D and Connors B W 2004 A microelectrode/microelectronic hybrid device for brain implantable neuroprosthesis applications *IEEE Trans. Biomed. Eng.* **51** 1845–53

[5] Song Y K *et al* 2005 Development of a chipscale integrated microelectrode/microelectronic device for brain implantable, neuroengineering applications *IEEE Trans. Neural Syst. Rehabil. Eng.* **13** 220–6

[6] Henry C H 1980 Limiting efficiencies of ideal single and multiple energy gap terrestrial solar cells *J. Appl. Phys.* **51** 4494–500

[7] Takahashi K, Yamada S and Unno T High-efficiency AlGaAs/GaAs tandem solar cells U.D.C. 621.383.51: 523.9–7: [546.681'62'19 : 546.681'19]

[8] Yamaguchi M 1999 Physics and technologies of super-high-efficiency tandem solar cells *Semiconductors* **33** 961–4

[9] Takamoto T, Ikeda E, Agui T, Kurita H, Tanabe T, Tanaka S, Matsubara H, Mine Y, Takagishi S and Yamaguchi M 1997 *Proc. 26th IEEE Photovoltaic Specialists Conf.* p 1031

[10] Kandel E R, Schwartz J H and Jessell T M 1999 *Principle of Neural Science* 4th edn (Columbus, OH: McGraw-Hill) pp 675–86

[11] Leventhal D K and Durand D M 2004 Chronic measurement of the stimulation selectivity of the flat interface nerve electrode *IEEE Trans. Biomed. Eng.* **51** 1649–2004

[12] National Toxicology Program. NTP Toxicology and Carcinogenesis Studies of Gallium Arsenide (CAS No. 1303-00-0) in F344/N Rats and B6C3F1 Mice (Inhalation Studies) 2000 *Natl. Toxicol. Program Tech. Rep. Ser.* **492** 1–306
Tanaka A 2004 Toxicity of indium arsenide, gallium arsenide, and aluminium gallium arsenide *Toxicol. Appl. Pharmacol.* **198** 405–11

[13] Eckhardt H, Cuomo J J, Guarnieri C R, Sakhrani V, Nagle H T and Ufer S 2002 Insulating barrier coatings for flexible ribbon cables and microelectrodes suitable for implantable devices *Adv. Microelectron.* **29** 10–11